Spring 5-2-2014

A First-Principles Examination of Dopants in HfO2

Daniel Cunningham
University of Connecticut - Storrs, djcunningham0@gmail.com

A First-Principles Examination of Dopants in HfO_2

Daniel Cunningham

University of Connecticut
Department of Materials Science and Engineering
Honors Thesis
May 2014

Honors Thesis Advisor: Dr. Rampi Ramprasad

Table of Contents

Abstract

A systematic first-principles study using density functional theory was performed on dopants in HfO_2, a material with great importance as a high-*k* dielectric. Sixteen dopants were tested, most of which came from the fourth period of the periodic table (K-Ge, Al and Si). The relative stability of the monoclinic, tetragonal, and cubic phases were calculated for HfO_2 with each dopant in order to determine which dopants tend to stabilize which phases. It was found that the most important factor in determining relative phase stability of doped HfO_2 was the ionic radius of the dopant, where dopants smaller than Hf tend to stabilize the tetragonal phase and dopants larger than Hf tend to stabilize the cubic phase. The results and methods of this study show a viable computational way to select dopants in HfO_2 or in other materials.

Acknowledgments

First and foremost, I would like to thank my Honors thesis advisor, Dr. Rampi Ramprasad. He originally introduced me to the field of computational materials science and quantum mechanical modeling. He was extremely helpful and supportive over the course of the entire year, as he helped me learn all of the necessary theory and background for the project and was always available for discussion. His knowledge of and passion for his field and his research is inspiring and I could not have hoped for a better advisor.

I would also like to thank all of Dr. Ramprasad's group members, especially Chenchen Wang and Vinit Sharma. They helped me learn how to actually run calculations and were always able to answer any questions I had.

Lastly, I would like to thank the faculty, staff, and students in the Materials Science and Engineering program. Our program is very supportive of its students and many people helped me over my four years at UConn and allowed me to get to this point.

List of Figures

List of Tables

1 Introduction

1.1 HfO_2 as gate dielectric

Hafnium oxide (HfO_2), or hafnia, is a dielectric material with several applications. Perhaps the most important contemporary application of hafnia is as an emerging replacement for the silicon dioxide (SiO_2) as the gate dielectric material in metal-oxide-semiconductor field-effect-transistors (MOSFETs). A MOSFET consists of several layers, including a metal gate electrode, a gate dielectric, and a semiconductor substrate, as seen in Figure 1. Si and SiO_2 are commonly used as the substrate and gate dielectric material, respectively. As MOSFETs become smaller, following the trend of Moore's Law, the capacitance of the gate dielectric must remain the same. Since capacitance varies with the thickness of a material, the gate dielectric must become thinner as devices become smaller. However, there comes a point when the oxide layer cannot be made any thinner. When an SiO_2 layer is about 1 nm thick, the leakage current due to quantum tunneling of electrons becomes too high. The absolute limiting thickness of an SiO_2 layer is about 7 Å, at which point SiO_2 loses its bulk behavior, such as its full energy gap [1]. The limiting thickness has very nearly been reached with SiO_2 as the gate dielectric material [2] , so a different approach must be taken in order to continue the advancement of MOSFET technology.

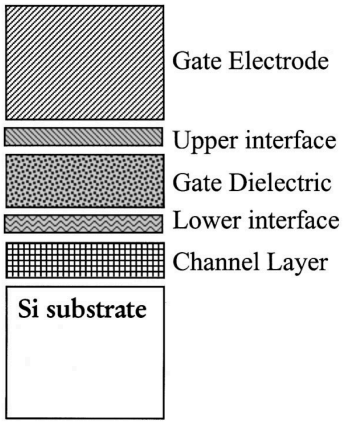

Figure 1: A schematic diagram of a MOSFET [3].

One potential approach is the use of high-*k* dielectrics, where *k* stands for the dielectric constant of a material. A material with a high dielectric constant can have a higher thickness while maintaining the same capacitance as a material with a low dielectric constant. If such a material were used as the gate dielectric in a MOSFET, the transistor could become smaller before being limited by the thickness of the dielectric. One of the most promising high-*k* dielectrics is HfO_2, which has a dielectric constant of approximately 25 in an amorphous state compared to approximately 4 for SiO_2. HfO_2 is also a promising replacement for other reasons, such as a large enough band gap and favorable stability and interface quality with Si, compared to other high-*k* dielectrics [3].

Hafnia is also used in other applications that make use of its high melting point, chemical stability, and low thermal conductivity. For example, hafnia is often used as a refractory material and in thermal barrier coatings [4].

1.2 Crystal Structures of HfO_2

Hafnia has three stable crystal structures at atmospheric pressure. The stable low temperature phase is monoclinic (space group $P2_1/c$). At 1720°C a tetragonal phase becomes stable (space group $P4_2/nmc$) and at 2600°C a cubic phase becomes stable (space group $Fm3m$). The structure of each phase can be seen in Figure 2.

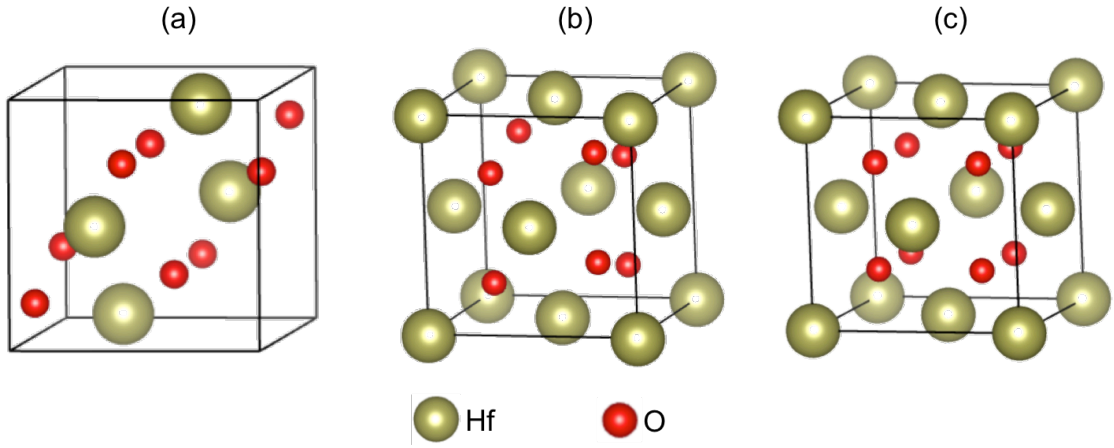

Figure 2: Standard 12-atom unit cells for HfO_2 in the (a) monoclinic, (b) tetragonal, and (c) cubic phases.

The different phases of hafnia have different properties. The monoclinic phase has the lowest dielectric constant of any of the phases (k = 16-18), while the cubic phase typically has a dielectric constant around 30 and the tetragonal phase has a dielectric constant calculated as high as 70 [5]. The phase of hafnia can also affect the quality of its interface with Si. The monoclinic phase typically has the least stable interface [6].

Other physical properties, such as bulk modulus and thermal conductivity, also change with the phase of hafnia. In particular, the cubic phase has a higher bulk modulus and a lower thermal conductivity than the other phases [7]. The low

thermal conductivity of the cubic phase makes it the most favorable phase for use in some applications, such as thermal barrier coatings for jet engines [4]. Since certain phases of hafnia can be more favorable for some applications, it is desirable to be able to change the relative stability of the three phases. One way of achieving this is through doping.

1.3 Dopants in HfO_2

Doping is the introduction of trace impurity elements in order to tune the properties of a material. It has been shown that certain dopants in hafnia can stabilize either the cubic or tetragonal phase over the monoclinic phase, which is typically stable at low temperatures. Many studies, both experimental and computational, have been performed on hafnia investigating the effect of a wide variety of dopants. It has been shown experimentally that some dopants, including Y, Gd, and Mn, stabilize the cubic phase at high enough dopant concentrations, typically around 10-20% [4, 8-10]. Computationally, it has been shown that dopants can stabilize either the cubic or tetragonal phase. One study in particular [11] found that some dopants (Si, Ge, Sn, Ti, P, Al) stabilize the tetragonal phase while others (Y, Sc, Gd) stabilize the cubic phase. This study identified the ionic radius as a property that affected the stable phase, where dopants with small ionic radii stabilize the tetragonal phase and dopants with large ionic radii stabilize the cubic phase.

Other interesting properties of doped hafnia have also been observed, unrelated to the relative stability of its phases. Experimentally, it has been shown that Gd-doped hafnia changes from an n-type to a p-type semiconductor with

increasing dopant concentration [8] and that Co-doped hafnia is paramagnetic [12]. Computationally, it has been predicted that Mn-doped hafnia is ferromagnetic and half-metallic, meaning it behaves as a conductor for electrons of one spin and an insulators for electrons with the opposite spin [13]. These studies are not particularly relevant to the current study, but they demonstrate some other types of properties that doping can affect and they show some potential future extensions or applications of this work.

1.4 Objectives of Research

The main objective of this study is to conduct a systematic examination of the role of dopants on the structure and relative stability of the phases of HfO_2. A large number of dopants were tested using modern quantum mechanical modeling techniques. This type of study is infeasible experimentally with such a high number of dopants in such a small time frame, and modern computational techniques have the predictive power necessary to yield valuable and accurate results. The dopants were chosen primarily from a single period from the periodic table, as seen in Figure 3. Dopants were chosen in this way so that trends in the data might be observed and used to find relationships between dopant properties and phase stability, analogous to the empirical Hume-Rothery rules for solid solutions.

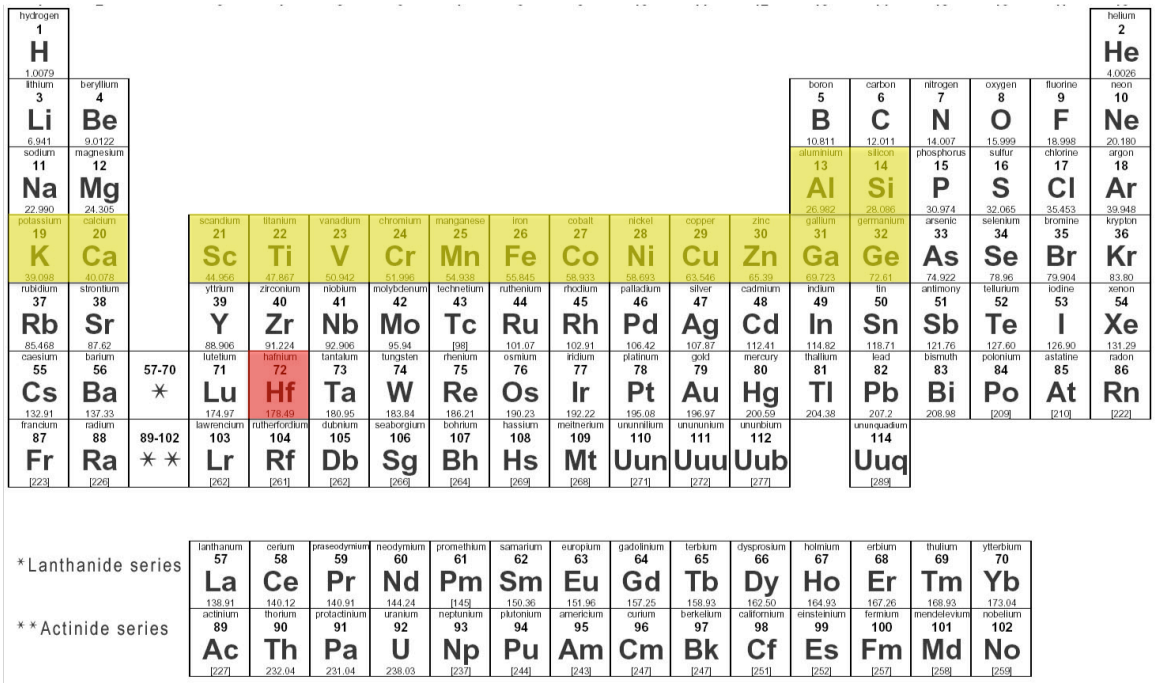

Figure 3: The dopants investigated in this study, highlighted in yellow. Hafnium is highlighted in red.

Another objective of this study is to develop and demonstrate a method for designing materials with desired properties through the use of first-principles modeling. A large number of calculations can be done on a wide variety of materials in order to create a comprehensive "library" of materials data. The creation of such a library would have a widespread impact on the field of materials science. The library would expedite the process of materials design by reducing the need for experimental testing and development. A similar computational study has previously been done on $BaTiO_3$ [14] and more studies are expected to be done in the future on other materials.

2 Computational Methods

2.1 Density Functional Theory

Density functional theory (DFT) is a first-principles method that is used to perform quantum mechanical modeling of many-body systems. DFT was first developed in the 1960s by Walter Kohn and others [15, 16]. It has since grown considerably in popularity. Today, DFT is used extensively in physics, chemistry, and materials science to model atoms, molecules, and solids containing up to a few hundred atoms.

The basis for DFT lies in quantum mechanics, specifically with the many-body Schrodinger equation. The Schrodinger equation is the most fundamental equation to quantum mechanics and it is written

$$H\Psi = E\Psi$$

where H is the Hamiltonian operator, Ψ is the wave function that describes the quantum state of the system, and E is the energy of the system. In a three-dimensional system with N electrons, Ψ is a function of $3N$ variables, the positions of each electron with three degrees of freedom. The many-electron Schrodinger equation is

$$H_{elec}\Psi(r_1, r_2, \dots, r_N) = E_{elec}\Psi(r_1, r_2, \dots r_N)$$

where each r_i represents the position of an electron in three dimensions. The Hamiltonian operator takes the form

$$H_{elec} = -\sum_{i=1}^{N} \frac{\hbar^2}{2m}\nabla_i^2 + \frac{1}{2}\sum_{i=1}^{N}\sum_{j\neq i}^{N} \frac{e^2}{|r_i - r_j|} - \sum_{I=1}^{M}\sum_{i=1}^{N} \frac{Z_I e^2}{|R_I - r_i|}$$

where the terms from left to right represent the kinetic energy of the electrons, the electron-electron interaction energy, and the potential energy from the external field from the positively charged nuclei. This equation quickly becomes impossible to solve analytically and extremely difficult to solve numerically as the size of the system increases due to the large number of variables.

DFT provides a more feasible way to solve such electronic structure problems. The key ideas behind DFT are the two Hohenberg-Kohn theorems [15]. The first Hohenberg-Kohn theorem states that the ground state energy from the many-electron Schrodinger equation is a unique functional of the electron density of the system. Thus, the many-electron Schrodinger problem, which depends on the wave functions of all electrons involved, can be mapped to a problem that depends only on the charge density $n(r)$ of the system without electron-electron interactions. By looking at this problem instead, it becomes necessary to find a function of three variables, $n(r)$, rather than a function of $3N$ variables, $\Psi(r_1, r_2, \dots, r_N)$. This first theorem implies that if the ground state electron density is known, then wave function (along with all properties of the system) is also known.

The second Hohenberg-Kohn theorem [16] provides more information about the functional of electron density. This theorem states that the electron density that minimizes the energy functional proven to exist by the first theorem is the true ground state electron density of the system. Thus, it becomes a minimization problem to determine the ground state electron density or, equivalently, the ground state energy. Using the assumptions of DFT, it can be shown that the ground state energy of the system is related to the ground state electron density by the equation

$$E_{elec} = T[n(r)] + \frac{e^2}{2}\iint \frac{n(r)n(r')}{|r-r'|} d^3r d^3r' + \int V(r)n(r)d^3r + E_{XC}[n(r)]$$

where the terms from left to right represent the electron kinetic energies, the Coulomb interactions between pairs of electrons, the Coulomb interactions between electrons and nuclei, and a term called the exchange correlation functional. All terms except the exchange correlation term are known and can be calculated more or less exactly. The exchange correlation functional is defined to include all quantum mechanical effects that are not accounted for by the other terms. In theory, DFT represents an exact solution of the many-body Schrodinger equation, but in practice the exact form of the exchange correlation functional is not known.

DFT does not provide a way to find the exact functional form of the exchange correlation interaction, so approximations must be used. Many approximations of various complexity for the exchange correlation functional have been developed. The simplest approximation of the exchange correlation is the local density approximation (LDA). This approximation uses only the local electron density to approximate the exchange correlation functional. The next step above LDA is the generalized gradient approximation (GGA). In addition to using local electron density, GGA uses the gradient of the local electron density to approximate the exchange correlation. It is possible to use more complex approximations by adding additional information, such as the second or third gradients of local electron density.

2.2 Details of Study

All calculations in this study were performed with the Vienna ab initio simulation package (VASP). The exchange correlation interaction was treated with the generalized gradient approximation (GGA) using the Perdew-Burke-Ernzerhoff (PBE) functional.

Before dopants were examined, DFT calculations were performed on bulk hafnia. First, convergence tests were performed in order to determine the choice of necessary parameters such as the size of the k-point mesh and the plane wave cutoff energy for all calculations. These convergence tests were performed on 12-atom unit cells of each of the three phases of HfO_2. Both the k-point and energy cutoff convergence tests were performed in order to obtain an energy value converged within 0.02 eV. It was found that 4 k-points in each direction (i.e., a $4 \times 4 \times 4$ Monkhorst-Pack mesh) and a plane wave cutoff energy of 600 eV were sufficient, as seen in Figure 4.

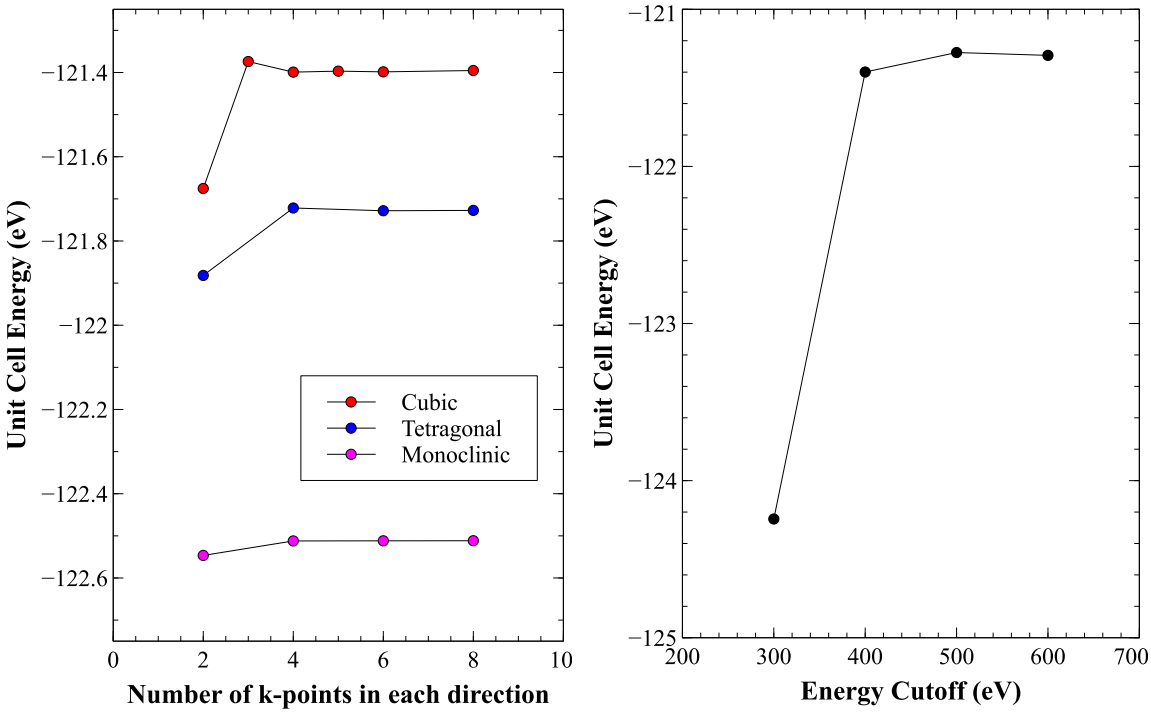

Figure 4: The k-point convergence (left) tests for the unit cells of all three phases of HfO_2 and the plane wave energy cutoff convergence test (right) performed on a cubic unit cell. It was found that a $4 \times 4 \times 4$ k-point mesh and a 600 eV energy cutoff gave sufficient accuracy for a 12-atom unit cell.

After the k-point mesh and plane wave cutoff energy were determined, the structural parameters of each phase of HfO_2 were calculated. For each crystal structure, the cell volume and parameters and the ion positions within the cell were allowed to relax in order to minimize the energy of the structure. The structural parameters of each relaxed structure were calculated. The calculated values are reported in Table 1, where they are compared with experimental data and other computational studies. The values calculated in the present study agree very well with the values from other sources.

	Present Study	Other theory (GGA)[a]	Other theory (LDA)[b]	Experiment[c]
Cubic				
a	5.06	5.05	5.04	5.08
Tetragonal				
a	5.07	5.06	5.06	5.15
c	5.20	5.20	5.13	5.29
Monoclinic				
a	5.14	5.12	5.11	5.12
b	5.19	5.20	5.17	5.17
c	5.32	5.28	5.28	5.30
beta	99.7	99.7	99.4	99.2

[a] Reference [11]
[b] Reference [17]
[c] Reference [18] (cubic, tetragonal) and Reference [19] (monoclinic)

Table 1: Calculated structural parameters and comparison to other theory and experimental values.

After the accuracy of the structural calculations had been confirmed by comparing with existing data, calculations with dopants were performed. All calculations with dopants were done using 2×2×2 supercells containing a total of eight HfO_2 unit cells (96 total atoms). Supercells were constructed by expanding the unit cell for a given phase twice in each direction. Since the size of the cell was doubled in each direction, the necessary number of k-points in each direction was halved. Thus, supercell calculations were performed using a 2×2×2 Monkhorst-Pack k-point mesh.

Dopants from across the periodic table (see Figure 3) were put into the supercells, with a single dopant atom replacing a single Hf atom. Each supercell contains 96 atoms with 32 Hf sites and 64 O sites, so the dopant concentration for

all calculations was 3.125% with respect to Hf. The generic doped supercells for each phase are shown in Figure 5.

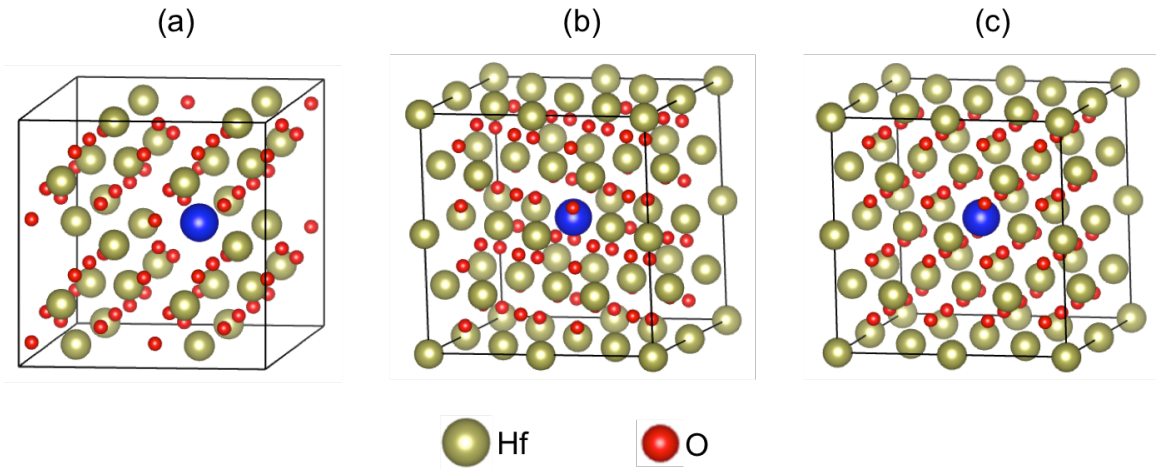

Figure 5: Supercells of HfO_2 containing one dopant atom (blue) in the (a) monoclinic, (b) tetragonal, and (c) cubic phases.

The supercells of doped HfO_2 were relaxed in exactly the same manner as described above for the structural calculations of the unit cells. The ion locations and cell volume were relaxed until the minimum energy configuration was found. These structural calculations were performed for all dopants in Figure 3 in each of the three phases of hafnia.

2.3 Calculation and Definitions of Relative Energies

When a structural calculation was performed with DFT, the equilibrium energy of the relaxed structure was calculated. Using this equilibrium energy, several relative energies were defined in order compare different doped structures with each other and with the undoped structures. For each dopant (and for undoped HfO_2), three DFT energies were calculated: the energies for the monoclinic, tetragonal, and cubic phases. The relative values of those energies compared to one

another are more meaningful than the actual values. Since the monoclinic structure is the stable low-temperature phase, it had the lowest equilibrium energy. The first set of relative energies was calculated by finding the difference between the monoclinic and the tetragonal or cubic phases. Thus, the relative tetragonal energy was defined as

$$\Delta E^{D}_{t-m} = E^{D}_{tetragonal} - E^{D}_{monoclinic}$$

and the relative cubic energy was defined as

$$\Delta E^{D}_{c-m} = E^{D}_{cubic} - E^{D}_{monoclinic},$$

where $E^{D}_{tetragonal}$ and E^{D}_{cubic} are the DFT energies of the relaxed structures of HfO_2 doped with the dopant D in the tetragonal and cubic phases, respectively. The relative energies for undoped hafnia were defined as ΔE^{Hf}_{t-m} and ΔE^{Hf}_{c-m}.

If $\Delta E^{D}_{t-m} < \Delta E^{Hf}_{t-m}$ for some dopant D, then D tends to stabilize the tetragonal phase (or the cubic phase if $\Delta E^{D}_{c-m} < \Delta E^{Hf}_{c-m}$). In order to more clearly visualize which dopants stabilize (and destabilize) which phase, a second set of relative energies was developed using the first set of relative energies. These relative energies are defined as $\Delta E^{D}_{t-m} - \Delta E^{Hf}_{t-m}$ and $\Delta E^{D}_{c-m} - \Delta E^{Hf}_{c-m}$ for the tetragonal and cubic phases, respectively. If $\Delta E^{D}_{t-m} - \Delta E^{Hf}_{t-m} < 0$ (or $\Delta E^{D}_{c-m} - \Delta E^{Hf}_{c-m} < 0$), then the dopant D tends to stabilize the tetragonal (or cubic) phase.

The relative energies were plotted against two dopant properties: ionic radius and oxidation state. The values used for ionic radius [20] and oxidation state of each dopant were the appropriate values for the most stable 0 K oxide of that dopant. Ionic radius and oxidations state were chosen because previous research

has shown strong trends between these properties and relative stability of structures [14].

3 Results and Discussion

Dopant	Ionic Radius (Å)	Oxidation State	ΔE_{t-m}^{D} (eV)	ΔE_{c-m}^{D} (eV)	$\Delta E_{t-m}^{D} - \Delta E_{t-m}^{Hf}$	$\Delta E_{c-m}^{D} - \Delta E_{c-m}^{Hf}$
Hf (pure)	0.71	+4	5.479	8.013	0.000	0.000
K	1.64	+1	5.378	7.453	-0.101	-0.560
Ca	1.34	+2	5.517	7.428	0.038	-0.585
Sc	0.75	+3	5.704	7.891	0.226	-0.122
Ti	0.61	+4	5.286	8.502	-0.192	0.490
V	0.58	+4	5.077	8.494	-0.401	0.481
Cr	0.55	+4	5.458	8.072	-0.021	0.059
Mn	0.53	+4	5.162	9.571	-0.317	1.559
Fe	0.65	+3	5.950	8.903	0.471	0.890
Co	0.53	+2	5.163	8.580	-0.316	0.567
Ni	0.69	+2	5.652	8.538	0.174	0.525
Cu	0.77	+2	5.482	7.921	0.003	-0.092
Zn	0.74	+2	5.366	7.820	-0.113	-0.193
Ga	0.62	+3	5.085	8.416	-0.394	0.403
Ge	0.53	+4	4.487	9.129	-0.991	1.116
Al	0.54	+3	4.967	8.706	-0.512	0.693
Si	0.40	+4	3.828	10.315	-1.651	2.302

[a] Reference [20]

Table 2: A summary of dopant properties and calculated values.

After calculations were run for each dopant in each phase of HfO_2, the relative energies were calculated for each dopant as described in Section 2.3. The relative energies and the dopant properties (ionic radius and oxidation state) are

reported in Table 2. The relative energies ΔE_{t-m}^{D} and ΔE_{c-m}^{D} were plotted against the dopants in order to visualize trends moving across the periodic table. This plot is shown in Figure 6. Other computational data is included when available for comparison [11]. The strong agreement between the present study and existing data suggests that the current calculations are accurate and reliable. The leftmost data point in each series on this plot represents pure HfO_2. Moving to the right, the period 4 dopants are shown in order followed by Al and Si. Data points connected by a solid line represent dopants adjacent to each other on the periodic table. In this plot, if a data point falls below the horizontal dashed line for either the relative cubic or tetragonal phase, then that dopant tends to stabilize that phase relative to the monoclinic phase. It becomes clear from Figure 6 that dopants that tend to stabilize either the cubic or tetragonal phase usually tend to destabilize the other phase.

It should be noted that none of the dopants changed the relative 0 K stability of the phases. For each dopant, the most stable (lowest energy) phase was the monoclinic phase, followed by the tetragonal phase, and finally the cubic phase. If a dopant tended to stabilize either the cubic or tetragonal phase, then the energy of that phase was lowered relative to the monoclinic phase without actually dropping below the energy of the monoclinic phase. The dopant concentration in this study was 3.125% with respect to Hf. It is expected that at higher dopant concentrations, a higher degree of stabilization (or destabilization) would occur. For example, Si stabilized the tetragonal phase more than any other dopant in this study. This result was expected because Si strongly prefers a tetrahedral environment, which is present in the tetragonal phase of HfO_2. At some higher dopant concentration (say,

around 10-15%), Si may stabilize the tetragonal phase to the point where the tetragonal phase is more stable than the monoclinic phase. I has been shown experimentally that mixing HfO_2 with 10% SiO_2 can fully stabilize the tetragonal phase [21].

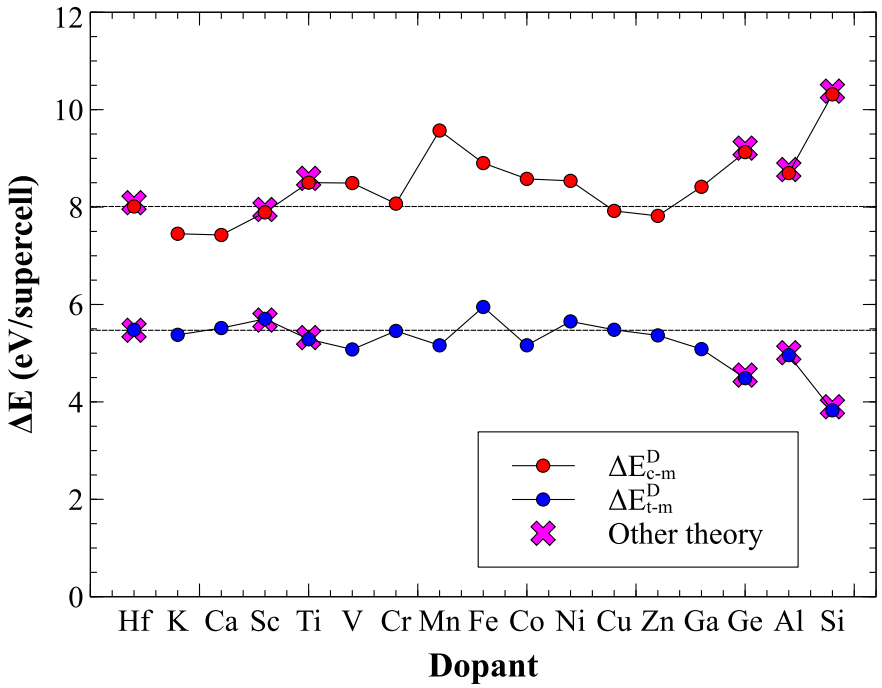

Figure 6: A plot of ΔE^D_{c-m} and ΔE^D_{t-m} for each dopant studied. The horizontal dotted lines correspond to ΔE^{Hf}_{c-m} and ΔE^{Hf}_{t-m}. Other theory data is from Reference [11].

In the next series of plots, the second set of relative energies, $\Delta E^D_{t-m} - \Delta E^{Hf}_{t-m}$ and $\Delta E^D_{c-m} - \Delta E^{Hf}_{c-m}$, were plotted against the properties of the dopants. The objective of these plots was to visualize how certain properties affect the relative stability of the phases, if at all. If clear trends emerge from these plots, they could be used to predict the effect of other dopants in HfO_2 based on their known properties.

The first property examined was ionic radius. Figure 7 shows a plot of $\Delta E^D_{t-m} - \Delta E^{Hf}_{t-m}$ and $\Delta E^D_{c-m} - \Delta E^{Hf}_{c-m}$ against a relative measure of ionic radius,

defined as $(r_D - r_{Hf})/r_{Hf}$, where r_D is the ionic radius of a dopant and $r_{Hf} = 0.71$ Å is the ionic radius of Hf. Note, by this metric the relative radius of Hf is zero. In Figure 7, points to the left of the vertical dotted line represent dopants with a smaller ionic radius than Hf and points to the right represent dopants with a larger ionic radius. If a point has a negative relative energy value (below the horizontal dotted line), then that phase tends to be stabilized, as explained in Section 2.3. There is a very clear trend that dopants with a smaller ionic radius tend to stabilize the tetragonal phase and destabilize the cubic phase. The smaller the ionic radius of the dopant relative to Hf, the more the tetragonal phase is stabilized. It also appears that dopants with larger ionic radii tend to stabilize the cubic phase. This trend is less clear because this region of the plot is less populated. More dopants with larger ionic radii than Hf should be examined in order to confirm this trend.

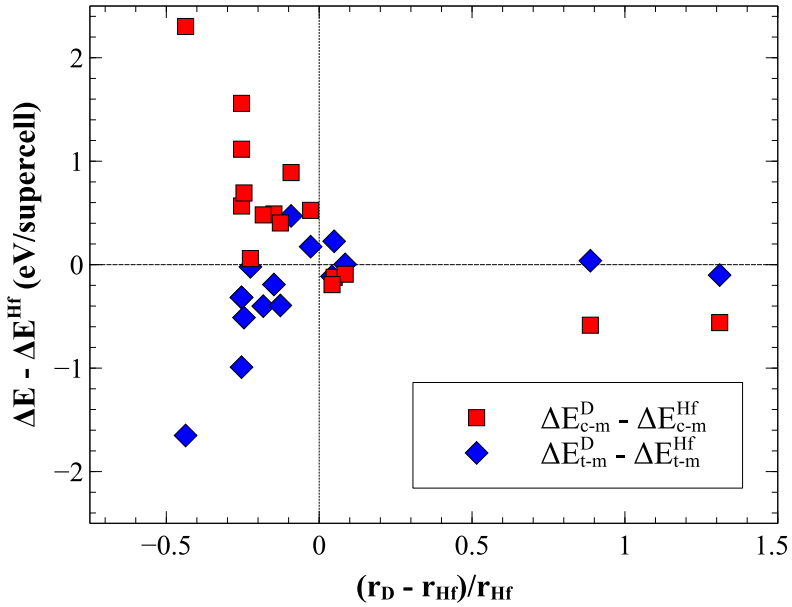

Figure 7: A plot of $\Delta E^D_{c-m} - \Delta E^{Hf}_{c-m}$ and $\Delta E^D_{t-m} - \Delta E^{Hf}_{t-m}$ against the relative ionic radius of each dopant compared to Hf. The horizontal and vertical dotted lines represent the values for pure HfO_2 and intercept their respective axes at zero.

The trend that smaller dopants tend to stabilize the tetragonal phase and larger dopants tend to stabilize the cubic phase was observed in another computational study on dopants in HfO_2 [11]. The present study confirms that trend and provides stronger evidence for it. Our study also examines more dopants and chooses them in a more systematic manner by moving across a period of the periodic table, which gives more reliability to the trend. Some overlap of dopants between the two studies occurred. For the dopants that were tested in both studies (Sc, Ti, Ge, Al, Si), the same results were obtained with respect to the stabilization of the tetragonal or cubic phases.

The second dopant property examined was oxidation state. Figure 8 shows a plot of $\Delta E^{D}_{t-m} - \Delta E^{Hf}_{t-m}$ and $\Delta E^{D}_{c-m} - \Delta E^{Hf}_{c-m}$ against oxidation state. Once again, data points below the horizontal line represent a dopant that tends to stabilize the given phase. Trends in this plot are not as clear as they were in the plot against ionic radius, but some observations can be made. It is clear that dopants whose most stable oxide has a +4 oxidation state, the same oxidation state as Hf, tend to stabilize the tetragonal phase. All dopants tested with oxidation state +4 tended to stabilize the tetragonal phase and destabilize the cubic phase. As the oxidation state moved further from the oxidation state of Hf, the cubic phase tended to be stabilized. However, this validity of this trend is questionable. A small number of dopants with oxidation states of +1 or +2 were tested compared with dopants with oxidation states of +3 or +4. Also, the only dopant tested with oxidation state +1 (K) tended to stabilize both the cubic and tetragonal phase. This observation casts some doubt on

the true nature of the relationship between dopant oxidation state and the relative stability of the doped HfO_2 phases.

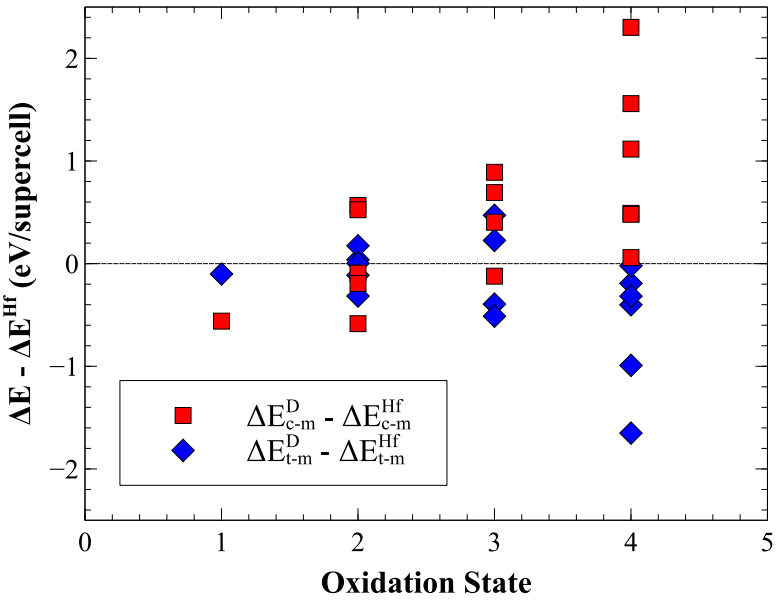

Figure 8: A plot of $\Delta E^{D}_{c-m} - \Delta E^{Hf}_{c-m}$ and $\Delta E^{D}_{t-m} - \Delta E^{Hf}_{t-m}$ against the oxidation state for all dopants. Dopants with oxidation states closest to that of Hf (+4) tend to stabilize the tetragonal phase and destabilize the cubic phase.

4 Conclusions and Outlook

4.1 Summary

A systematic examination of dopants in HfO_2 was performed using state-of-the-art first-principles computations and trends were found between the properties of the dopants and the relative stability of the different structures. Of the two properties examined in this study, the ionic radius of a dopant appears to correlate more strongly with phase stabilization data than oxidation state. A similar result was found in previous research within the group on $BaTiO_3$ [14], which considered

the dopant formation energy. In that study it was found that ionic radius was the most important property for determining the favored dopant site (Ba or Ti), followed by oxidation state.

The method used in this study has the potential to be applied to other material systems. Other systematic studies can be done following almost an identical procedure to create data that can be used for materials selection and design experiments. The relative energies defined in this study might be directly applicable to future studies or might be able to be modified to meet the needs of a particular study.

4.2 Future Directions

The work done in this study could be continued in several future directions. The most straightforward future direction is to continue the exact same study to examine more dopants. In particular, the elements across periods 5 and 6 of the periodic table could be tested as dopants in order to verify the results found with the period 4 elements in this study. More data is especially needed for elements with larger ionic radii than Hf, as the majority of dopants considered in this study had smaller ionic radii. Another future direction that should be taken to continue this study is the examination of oxygen vacancies. Some dopants replacing a Hf ion in HfO_2 may be more stable (lower energy) when accompanied by a neighboring O vacancy. This is especially likely to be the case for dopants with lower oxidation states than Hf, several of which were studied in this work. For example, a dopant

with a +2 oxidation state replacing a Hf atom (+4 oxidation state) can be expected to be accompanied by an O^{2-} vacancy to preserve charge neutrality. A well-known example of this phenomenon occurs in yttria-doped zirconia. In this case, the when two Y^{3+} replace two Zr^{4+} atoms in the zirconia lattice, an oxygen vacancy is formed. Hafnia has a nearly identical structure to zirconia, so a similar result is expected. In order to complete this study, oxygen vacancies must be considered.

A future direction that represents an extension rather than a continuation of this work would be to look at the effect of higher dopant concentrations. The dopant concentration in this study (3.125%) was too low to change the relative stability of the 0 K phases of hafnia. That is, the monoclinic phase was most stable, followed by the tetragonal phase and then the cubic phase for each dopant. It is expected that at some higher dopant concentrations, certain dopants would be able to change the most stable 0 K phase of hafnia. For example, Si is expected to stabilize the tetragonal phase over the monoclinic phase at some dopant concentration, probably in the range of 10-15%. A future study could be performed on Si-doped hafnia to pinpoint exactly what the dopant concentration must be for the switch to occur.

Another possible extension of this study would be to confirm other types of properties observed in doped hafnia, as described in Section 1.3. For example, the electronic band structures could be calculated in order to confirm whether Mn-doped HfO_2 is half-metallic [13] or Co-doped HfO_2 is paramagnetic [12]. In addition to confirming existing experimental and theoretical work, new properties might be discovered for some dopants in hafnia.

4.3 Reflections

This Honors Thesis gave me the opportunity to experience academic research in the very exciting field of computational materials science. I wanted to work on a project more on the theoretical side of materials science, different from the typical work we do within the curriculum, and I am very glad I ended up working with Dr. Ramprasad and his research group. I was fortunate to work with a group of smart and supportive people who helped me over the course of the year when I had questions. It was a learning experience throughout the entire year, from learning the basics of DFT and VASP in the fall semester to learning how to run calculations and analyze the results in the spring. I was able to learn about and actively participate in one of the most interesting fields of materials science, and I am very thankful for that opportunity.

5 References

1. Muller, D.A., et al., *The electronic structure at the atomic scale of ultrathin gate oxides.* Nature, 1999. **399**(6738): p. 758-761.
2. Chau, R., et al., *Integrated nanoelectronics for the future.* Nat Mater, 2007. **6**(11): p. 810-812.
3. Wilk, G.D., R.M. Wallace, and J.M. Anthony, *High-kappa gate dielectrics: Current status and materials properties considerations.* Journal of Applied Physics, 2001. **89**(10): p. 5243-5275.
4. Matovic, B., et al., *Synthesis and characterization of nanometric yttrium-doped hafnia solid solutions.* Journal of the European Ceramic Society, 2012. **32**(9): p. 1971-1976.
5. Zhao, X. and D. Vanderbilt, *First-principles Study of Electronic and Dielectric Properties of ZrO2 and HfO2.* MRS Online Proceedings Library, 2002. **747**: p. null-null.
6. Tang, C., *First principles studies of point defects in HfO2 and Si-HfO2 interfaces.* Doctoral Dissertations, 2009. **Paper AAI3383932**.
7. Debernardi, A., *Ab initio study of phase transition and dielectric constants of high-kappa HfO2 as a function of Ge alloying.* Physical Review B, 2012. **85**(2): p. 6.
8. Losovyj, Y.B., et al., *The electronic structure change with Gd doping of HfO2 on silicon.* Applied Physics Letters, 2007. **91**(13): p. 3.
9. Gao, L., et al., *Stabilization of cubic structure in Mn-doped hafnia.* Ceramics International, 2012. **38**(3): p. 2305-2311.
10. Ortega, A., et al., *Correlation between phase and optical properties of yttrium-doped hafnium oxide nanocrystalline thin films.* Optical Materials, 2013. **35**(9): p. 1728-1734.
11. Lee, C.K., et al., *First-principles study on doping and phase stability of HfO2.* Physical Review B, 2008. **78**(1): p. 4.
12. Buha, J., et al., *Solvothermal and surfactant-free synthesis of crystalline Nb2O5, Ta2O5, HfO2, and Co-doped HfO2 nanoparticles.* Physical Chemistry Chemical Physics, 2010. **12**(47): p. 15537-15543.
13. Maznichenko, I.V., et al., *First-principles study of manganese-stabilized hafnia.* Journal of Magnetism and Magnetic Materials, 2009. **321**(7): p. 913-916.
14. Sharma, V., et al., *Comprehensive examination of dopants and defects in BaTiO3 from first principles.* Physical Review B, 2013. **87**(13): p. 7.
15. Hohenberg, P. and W. Kohn, *Inhomogeneous Electron Gas.* Physical Review, 1964. **136**(3B): p. B864-B871.
16. Kohn, W. and L.J. Sham, *Self-Consistent Equations Including Exchange and Correlation Effects.* Physical Review, 1965. **140**(4A): p. A1133-A1138.
17. Zhao, X.Y. and D. Vanderbilt, *First-principles study of structural, vibrational, and lattice dielectric properties of hafnium oxide.* Physical Review B, 2002. **65**(23): p. 4.
18. Wang, J., H.P. Li, and R. Stevens, *HAFNIA AND HAFNIA-TOUGHENED CERAMICS.* Journal of Materials Science, 1992. **27**(20): p. 5397-5430.

19. Adam, J. and M.D. Rogers, *The crystal structure of ZrO2 and HfO2.* Acta Crystallographica, 1959. **12**(11): p. 951.
20. Shannon, R.D., *REVISED EFFECTIVE IONIC-RADII AND SYSTEMATIC STUDIES OF INTERATOMIC DISTANCES IN HALIDES AND CHALCOGENIDES.* Acta Crystallographica Section A, 1976. **32**(SEP1): p. 751-767.
21. Böscke, T.S., et al., *Stabilization of higher-κ tetragonal HfO2 by SiO2 admixture enabling thermally stable metal-insulator-metal capacitors.* Applied Physics Letters, 2007. **91**(7): p. -.